Conformational Characteristics of Poly(tetramethylene oxide)

Robert V. Law[†,‡] and Yuji Sasanuma*[,†]

Department of Polymer Physics, National Institute of Materials and Chemical Research (NIMC), 1-1 Higashi, Tsukuba, Ibaraki 305-8565, Japan, Department of Chemistry, Imperial College of Science, Technology and Medicine, London SW7 2AY, U.K., Department of Applied Chemistry, Faculty of Engineering, Chiba University, 1-33 Yayoicho, Inageku, Chiba 263-8522, Japan

Received August 15, 1997; Revised Manuscript Received December 20, 1997

ABSTRACT: Conformational characteristics of poly(tetramethylene oxide) (PTMO) have been investigated on the basis of the conformational energies evaluated for its monomer model 1,4-dimethoxybutane (DMB) from the ab initio molecular orbital (MO) calculations at the second-order Møller−Plesset correlation level with the 6-31+G* basis set. The reliability of our conformational energies was examined by comparison between calculations and observations of NMR vicinal $^{13}C-^{1}H$ and $^{1}H-^{1}H$ coupling constants of DMB and the characteristic ratio and dipole moment ratio of PTMO. Then the C−O bond dipole moment (m_{C-O}) for the rotational isomeric state analysis of polyethers was determined from the MO and ^{1}H NMR data reported previously for 1,2-dimethoxypropane, a monomeric model compound of poly(propylene oxide). The optimal m_{C-O} value was obtained as 1.18 D. The conformational energies reproduced the experimental observations very well. The relationship between the conformational characteristics and crystal structures of polyethers $[-(CH_2)_y-O-]_x$ ($y \geq 4$) is also discussed.

Introduction

Polyethers often exhibit the gauche preference about the C−C skeletal bond adjacent to the oxygen atom.[1−4] Recently, some of these phenomena have been interpreted in terms of the intramolecular interaction found by ab initio molecular orbital (MO) calculations. For poly(ethylene oxide), e.g., the nonbonded (C−H)···O interaction occurring in the $g^{\pm}g^{\mp}$ conformations for the C−O/C−C bond pair was suggested to stabilize the gauche state of the C−C bond.[5,6] In our previous study[7] the gauche stability for the C−C skeletal bond of poly(propylene oxide) (PPO) was also indicated to arise from the intramolecular (C−H)···O attractions. As an example of such interactions, illustrated in Figure 1 is 2,6-(C−H)···O hydrogen bond of 1,4-dimethoxybutane (DMB),[8] which corresponds to a monomeric model compound of poly(tetramethylene oxide) (PTMO) treated here.

To elucidate the nature of the (C−H)···O interactions, we have carried out the MO calculations for a series of dimethoxy ethers $CH_3O-(CH_2)_y-OCH_3$ ($y = 4-8$), which correspond to the higher homologues of 1,2-dimethoxyethane, a monomer model of poly(ethylene oxide), and model compounds of polyethers $[-(CH_2)_y-O-]_x$, and investigated the conformational free energies, the equilibrium geometries, and the partial charge distribution.[8] As a result, we have found the following facts. (1) The (C−H)···O interaction energy (E_ω) depends on the number of methylene units between the two oxygen atoms. For example, the MO calculations at the MP2/6-31+G*//HF/6-31G* (gas) level[9] yielded a negative E_ω value (−0.43 kcal mol^{-1}) only for DMB and positive values (0.24−0.66 kcal mol^{-1}) for the other longer ethers ($5 \leq y \leq 8$).[10] For $5 \leq y \leq 8$, the E_ω values are almost equivalent to those (0.3−0.6 kcal mol^{-1}) estimated from molecular mechanics calculations (cf. e.g., the E_ω values of studies I−III in Table 1). (2) The (C−H)···O interaction has an electrostatic character; the sign and magnitude of E_ω have a strong correlation with the partial charges on the oxygen atom and methylene group.

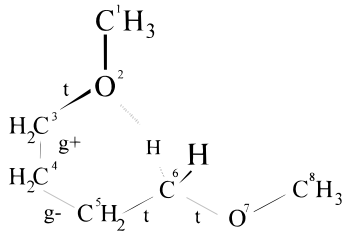

Figure 1. Nonbonded 2,6-(C−H)···O interaction formed in the tg^+g^-tt conformation of a monomer model of poly(tetramethylene oxide) (PTMO), 1,4-dimethoxybutane (DMB).

In Table 1 the conformational energies we obtained for DMB are compared with those reported so far for DMB and PTMO. Because we have no experimental data sufficient to elucidate the solvent dependence on the conformations of DMB and PTMO, we have not considered the solvent effects. In the previous study on PPO,[7] we have examined the validity of different combinations of electron correlation and basis set in the MO calculations. The MP2/6-31+G*//HF/6-31G* level gave the best results consistent with experiment. Thus we have employed only the MP2/6-31+G*//HF/6-31G* (gas) data in this study. From Table 1 it can be seen that our data are different from the others except for E_ρ: smaller $E_{\sigma 1}$, larger $E_{\sigma 2}$, and negative E_ω. The interaction energy E_ζ newly introduced will be explained later. It can also be found that the gauche stability of bond b of PTMO (bond 3 of DMB, see Figure 2) is suggested to be ascribed partly to the first-order interaction energy $E_{\sigma 1}$ and partly to the second-order E_ω. The former represents the attractive gauche effect,[13] and the latter, the (C−H)···O attraction.

* Author to whom correspondence should be addressed at Chiba University.

† This study was begun at NIMC and has been continued between the Imperial College of Science, Technology and Medicine and Chiba University after the authors left NIMC.

‡ Present address: Imperial College of Science, Technology and Medicine.

S0024-9297(97)01234-5 CCC: $15.00
Published on Web 03/13/1998

Table 1. Conformational Energies of DMB and PTMO: Comparison of the Present with Previous Studies[a]

	this study[b]	study I[c]	study II[d]	study III[e]
		First-Order Interaction		
E_ρ	0.829	0.90	0.90−1.2	1.0
$E_{\sigma 1}$	−0.648	−0.20	−0.25 to −0.15	−0.2 to −0.1
$E_{\sigma 2}$	0.832	0.50	0.50	0.3
		Second-Order Interaction		
E_ω	−0.430	0.34	0.60	0.47
		Third-Order Interaction		
E_ζ[f]	0.738			

[a] In kcal mol^{-1}. For the definition of the conformational energies, see Figure 2. The first-, second-, and third-order interactions depend on the relative positions of atoms and groups separated by three, four, and five bonds respectively, thus being considered a function of conformations of the intervening bonds. [b] Obtained by ab initio MO calculations at the MP2/6-31+G*//HF/6-31G* (gas) level. For details of the calculations, see ref 8. [c] Reference 2. [d] Reference 3. [e] Reference 12. [f] Due to the nonbonded 2,7-O···O interaction illustrated in Figure 4.

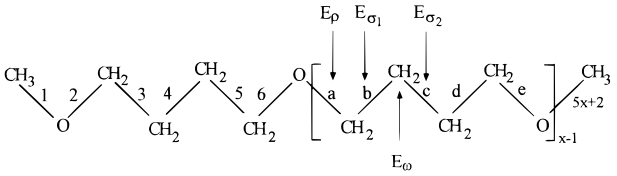

Figure 2. Schematic representation of DMB ($x = 1$) and PTMO (poly(tetramethylene oxide) dimethyl ether ($x \geq 2$)) with the definition of the conformational energies, where x is the degree of polymerization. As indicated, the bonds are numbered. The first-order interaction energies E_ρ, $E_{\sigma 1}$, and $E_{\sigma 2}$ are assigned to the $g^\pm$ states of the CO−CC (2, 6, a, and e), OC−CC (3, 5, b, and d) and CC−CC (4 and c) bonds respectively, and the second-order E_ω to the $g^\pm g^\mp$ states for the successive C−C/C−C bond pairs. The third-order interaction energy E_ζ introduced is illustrated in Figure 4.

In this paper the reliability of our conformational energy set is examined by comparison between calculations and observations of conformation-dependent properties such as NMR vicinal $^{13}C-^1H$ and $^1H-^1H$ coupling constants of DMB and the characteristic ratio and dipole moment ratio of PTMO, and furthermore, the crystal structures of polyethers $[-(CH_2)_y-O-]_x$ are discussed in relation to their conformational characteristics.

Statistical Weight Matrixes of DMB and PTMO

In previous conformational analyses of PTMO,[2,3,12] only the first- and second-order intramolecular interactions have been considered. Then all the statistical weight matrixes assigned to the skeletal bonds are 3×3.[14] In our rotational isomeric state (RIS) treatment, however, the third-order interactions have also been included, because inspection of the molecular models has indicated that some steric repulsions occur between groups separated by five bonds. The statistical weight matrixes of DMB ($x = 1$) and PTMO ($x \geq 2$) were formulated according to the 9×9 matrix scheme[15] as shown in Figure 3, where, for example, the statistical weight ρ is related to the corresponding conformational energy E_ρ by $\rho = \exp(-E_\rho/RT)$, R and T being the gas constant and absolute temperature, respectively. As a model for the RIS analysis, we have adopted poly(tetramethylene oxide) dimethyl ether depicted in Figure 2, because a 3-fold symmetrical rotation can be assumed for the terminal C−C bonds.

Severe third-order steric conflicts were found in some conformations, thus the corresponding elements in the U_i (i: bond number) matrixes were filled with zeros: $g^+g^-g^+$ and $g^-g^+g^-$ in U_4; $g^+g^-g^+$ and $g^-g^+g^-$ in U_5 (U_d); $g^+g^-g^-$ and $g^-g^+g^+$ in U_a; $g^+g^-g^-$ and $g^-g^+g^+$ in U_b; $g^+g^-g^+$, $g^+g^-g^-$, $g^-g^+g^+$, and $g^-g^+g^-$ in U_c. The elements for the $g^+g^+g^-$, $g^+g^-g^-$, $g^-g^+g^+$, and $g^-g^-g^+$ states of the U_5 and U_d matrixes include the new statistical weight ζ, which represents a third-order 2,7-O···O repulsion illustrated in Figure 4. The interaction energy E_ζ was evaluated to be 0.738 kcal mol^{-1} by subtracting $E_{\sigma 1} \times 2 + E_{\sigma 2} + E_\omega$ from the conformational free energies of the $tg^+g^+g^-t$ and $tg^+g^-g^-t$ states of DMB. Both conformers have the same statistical weights of $\sigma_1^2\sigma_2\omega\zeta$; the equilibrium $O^2\cdots O^7$ distance of 3.884 Å was obtained by the geometrical optimization at the HF/6-31G* level.

NMR Vicinal Coupling Constants of DMB

Experimental data of ^{13}C- and ^1H NMR vicinal coupling constants of DMB were reported by Inomata et al.[12] In our study, their data have been used. According to them, observed values of the $^{13}C-^1H$ ($^3J_{CH}$) (see Figure 5a), $^1H_\alpha-^1H_\beta$ ($^3J_{\alpha\beta}$) (b), and $^1H_\beta-^1H_\gamma$ or $^1H_{\beta'}-^1H_{\gamma'}$ ($^3J_{\beta\gamma}$) and $^1H_{\beta'}-^1H_\gamma$ or $^1H_\beta-^1H_{\gamma'}$ ($^3J'_{\beta\gamma}$) (c) coupling constants are respectively expressed as

$$^3J_{CH} = J_G\, p_{t;2} + (J_T + J'_G)p_{g+;2} \quad (1)$$

$$^3J_{\alpha\beta} = \frac{J_T + J_G}{2}p_{t;3} + \frac{J'_T + J'_G + J''_G + J'''_G}{2}p_{g+;3} \quad (2)$$

$$^3J_{\beta\gamma} = J_G\, p_{t;4} + (J'_T + J''_G)p_{g+;4} \quad (3)$$

$$^3J'_{\beta\gamma} = J_T\, p_{t;4} + 2J'_G\, p_{g+;4} \quad (4)$$

where $p_{\xi;i}$ represents the fraction (bond conformation) of the ξ (=t, g^+, or g^-) state of bond i ($i = 2-4$) and J_T, J'_T, J_G, J'_G, J''_G, and J'''_G are defined for each bond as shown in Figure 5. The fraction $p_{\xi;i}$ can be calculated from the statistical weight matrixes shown in Figure 3.[14]

The analysis of vicinal coupling constants is often carried out by using the J_T and J_G values obtained from, e.g., a rigid cyclic compound having a similar skeletal structure; the bond conformations are then treated as variables. In this study, however, the bond conformations were evaluated using our conformational energies listed in Table 1, and the J_T and J_G values were adjusted by the least-squares method[16] so as to give the best agreement between the calculated and observed coupling constants. Then we assumed that $J_T = J'_T$ and $J_G = J'_G = J''_G = J'''_G$.

The results of the simulations for $^3J_{CH}$ are shown in Figure 6, indicating good reproduction of the experimental observations. The J_T and J_G values were determined as 12.8 and 1.6 Hz (cyclohexane) and 13.1 and 1.8 Hz (DMSO), respectively. Inomata et al.[12] reported that the best agreement between theory and experiment was attained by a similar simulation using $J_T + J'_G = 16.0$ Hz and $J_G = 2.0$ Hz (if $J_G = J'_G$, $J_T = 14.0$ Hz, and $J_G = 2.0$ Hz).

In Figure 7 the calculated $^3J_{\alpha\beta}$, $^3J_{\beta\gamma}$, and $^3J'_{\beta\gamma}$ values are compared with the relevant observations. All the experimental data are found to be reproduced satisfactorily. The J_T and J_G values were determined as follows: for $^3J_{\alpha\beta}$, $J_T = 13.0$ Hz and $J_G = 3.3$ Hz

$$U_2 = \begin{array}{c} \\ t \\ g^+ \\ g^- \end{array} \begin{array}{c} \begin{array}{ccc} t & g^+ & g^- \end{array} \\ \begin{pmatrix} 1 & \rho & \rho \\ 0 & 0 & 0 \\ 0 & 0 & 0 \end{pmatrix} \end{array}$$

$$U_3 = \begin{array}{c} \\ t \\ g^+ \\ g^- \end{array} \begin{array}{c} \begin{array}{ccccccccc} t & g^+ & g^- & t & g^+ & g^- & t & g^+ & g^- \end{array} \\ \begin{pmatrix} 1 & \sigma_1 & \sigma_1 & 0 & 0 & 0 & 0 & 0 & 0 \\ 0 & 0 & 0 & 1 & \sigma_1 & 0 & 0 & 0 & 0 \\ 0 & 0 & 0 & 0 & 0 & 0 & 1 & 0 & \sigma_1 \end{pmatrix} \end{array}$$

$$U_4 = \begin{array}{c} \\ tt \\ tg^+ \\ tg^- \\ g^+t \\ g^+g^+ \\ g^+g^- \\ g^-t \\ g^-g^+ \\ g^-g^- \end{array} \begin{array}{c} \begin{array}{ccccccccc} t & g^+ & g^- & t & g^+ & g^- & t & g^+ & g^- \end{array} \\ \begin{pmatrix} 1 & \sigma_2 & \sigma_2 & 0 & 0 & 0 & 0 & 0 & 0 \\ 0 & 0 & 0 & 1 & \sigma_2 & \sigma_2\omega & 0 & 0 & 0 \\ 0 & 0 & 0 & 0 & 0 & 0 & 1 & \sigma_2\omega & \sigma_2 \\ 1 & \sigma_2 & \sigma_2 & 0 & 0 & 0 & 0 & 0 & 0 \\ 0 & 0 & 0 & 1 & \sigma_2 & \sigma_2\omega & 0 & 0 & 0 \\ 0 & 0 & 0 & 0 & 0 & 0 & 1 & 0 & \sigma_2 \\ 1 & \sigma_2 & \sigma_2 & 0 & 0 & 0 & 0 & 0 & 0 \\ 0 & 0 & 0 & 1 & \sigma_2 & 0 & 0 & 0 & 0 \\ 0 & 0 & 0 & 0 & 0 & 0 & 1 & \sigma_2\omega & \sigma_2 \end{pmatrix} \end{array}$$

$$U_5 = \begin{array}{c} \\ tt \\ tg^+ \\ tg^- \\ g^+t \\ g^+g^+ \\ g^+g^- \\ g^-t \\ g^-g^+ \\ g^-g^- \end{array} \begin{array}{c} \begin{array}{ccccccccc} t & g^+ & g^- & t & g^+ & g^- & t & g^+ & g^- \end{array} \\ \begin{pmatrix} 1 & \sigma_1 & \sigma_1 & 0 & 0 & 0 & 0 & 0 & 0 \\ 0 & 0 & 0 & 1 & \sigma_1 & \sigma_1\omega & 0 & 0 & 0 \\ 0 & 0 & 0 & 0 & 0 & 0 & 1 & \sigma_1\omega & \sigma_1 \\ 1 & \sigma_1 & \sigma_1 & 0 & 0 & 0 & 0 & 0 & 0 \\ 0 & 0 & 0 & 1 & \sigma_1 & \sigma_1\omega\zeta & 0 & 0 & 0 \\ 0 & 0 & 0 & 0 & 0 & 0 & 1 & 0 & \sigma_1\zeta \\ 1 & \sigma_1 & \sigma_1 & 0 & 0 & 0 & 0 & 0 & 0 \\ 0 & 0 & 0 & 1 & \sigma_1\zeta & 0 & 0 & 0 & 0 \\ 0 & 0 & 0 & 0 & 0 & 0 & 1 & \sigma_1\omega\zeta & \sigma_1 \end{pmatrix} \end{array}$$

$$U_6 = \begin{array}{c} \\ tt \\ tg^+ \\ tg^- \\ g^+t \\ g^+g^+ \\ g^+g^- \\ g^-t \\ g^-g^+ \\ g^-g^- \end{array} \begin{array}{c} \begin{array}{ccccccccc} t & g^+ & g^- & t & g^+ & g^- & t & g^+ & g^- \end{array} \\ \begin{pmatrix} 1 & \rho & \rho & 0 & 0 & 0 & 0 & 0 & 0 \\ 0 & 0 & 0 & 1 & \rho & 0 & 0 & 0 & 0 \\ 0 & 0 & 0 & 0 & 0 & 0 & 1 & 0 & \rho \\ 1 & \rho & \rho & 0 & 0 & 0 & 0 & 0 & 0 \\ 0 & 0 & 0 & 1 & \rho & 0 & 0 & 0 & 0 \\ 0 & 0 & 0 & 0 & 0 & 0 & 1 & 0 & \rho \\ 1 & \rho & \rho & 0 & 0 & 0 & 0 & 0 & 0 \\ 0 & 0 & 0 & 1 & \rho & 0 & 0 & 0 & 0 \\ 0 & 0 & 0 & 0 & 0 & 0 & 1 & 0 & \rho \end{pmatrix} \end{array}$$

$$U_a = \begin{array}{c} \\ tt \\ tg^+ \\ tg^- \\ g^+t \\ g^+g^+ \\ g^+g^- \\ g^-t \\ g^-g^+ \\ g^-g^- \end{array} \begin{array}{c} \begin{array}{ccccccccc} t & g^+ & g^- & t & g^+ & g^- & t & g^+ & g^- \end{array} \\ \begin{pmatrix} 1 & \rho & \rho & 0 & 0 & 0 & 0 & 0 & 0 \\ 0 & 0 & 0 & 1 & \rho & 0 & 0 & 0 & 0 \\ 0 & 0 & 0 & 0 & 0 & 0 & 1 & 0 & \rho \\ 1 & \rho & \rho & 0 & 0 & 0 & 0 & 0 & 0 \\ 0 & 0 & 0 & 1 & \rho & 0 & 0 & 0 & 0 \\ 0 & 0 & 0 & 0 & 0 & 0 & 1 & 0 & 0 \\ 1 & \rho & \rho & 0 & 0 & 0 & 0 & 0 & 0 \\ 0 & 0 & 0 & 1 & 0 & 0 & 0 & 0 & 0 \\ 0 & 0 & 0 & 0 & 0 & 0 & 1 & 0 & \rho \end{pmatrix} \end{array}$$

$$U_b = \begin{array}{c} \\ tt \\ tg^+ \\ tg^- \\ g^+t \\ g^+g^+ \\ g^+g^- \\ g^-t \\ g^-g^+ \\ g^-g^- \end{array} \begin{array}{c} \begin{array}{ccccccccc} t & g^+ & g^- & t & g^+ & g^- & t & g^+ & g^- \end{array} \\ \begin{pmatrix} 1 & \sigma_1 & \sigma_1 & 0 & 0 & 0 & 0 & 0 & 0 \\ 0 & 0 & 0 & 1 & \sigma_1 & 0 & 0 & 0 & 0 \\ 0 & 0 & 0 & 0 & 0 & 0 & 1 & 0 & \sigma_1 \\ 1 & \sigma_1 & \sigma_1 & 0 & 0 & 0 & 0 & 0 & 0 \\ 0 & 0 & 0 & 1 & \sigma_1 & 0 & 0 & 0 & 0 \\ 0 & 0 & 0 & 0 & 0 & 0 & 1 & 0 & 0 \\ 1 & \sigma_1 & \sigma_1 & 0 & 0 & 0 & 0 & 0 & 0 \\ 0 & 0 & 0 & 1 & 0 & 0 & 0 & 0 & 0 \\ 0 & 0 & 0 & 0 & 0 & 0 & 1 & 0 & \sigma_1 \end{pmatrix} \end{array}$$

$$U_c = \begin{array}{c} \\ tt \\ tg^+ \\ tg^- \\ g^+t \\ g^+g^+ \\ g^+g^- \\ g^-t \\ g^-g^+ \\ g^-g^- \end{array} \begin{array}{c} \begin{array}{ccccccccc} t & g^+ & g^- & t & g^+ & g^- & t & g^+ & g^- \end{array} \\ \begin{pmatrix} 1 & \sigma_2 & \sigma_2 & 0 & 0 & 0 & 0 & 0 & 0 \\ 0 & 0 & 0 & 1 & \sigma_2 & \sigma_2\omega & 0 & 0 & 0 \\ 0 & 0 & 0 & 0 & 0 & 0 & 1 & \sigma_2\omega & \sigma_2 \\ 1 & \sigma_2 & \sigma_2 & 0 & 0 & 0 & 0 & 0 & 0 \\ 0 & 0 & 0 & 1 & \sigma_2 & \sigma_2\omega & 0 & 0 & 0 \\ 0 & 0 & 0 & 0 & 0 & 0 & 1 & 0 & 0 \\ 1 & \sigma_2 & \sigma_2 & 0 & 0 & 0 & 0 & 0 & 0 \\ 0 & 0 & 0 & 1 & 0 & 0 & 0 & 0 & 0 \\ 0 & 0 & 0 & 0 & 0 & 0 & 1 & \sigma_2\omega & \sigma_2 \end{pmatrix} \end{array}$$

$$U_d = U_5$$

$$U_e = U_6$$

Figure 3. Statistical weight matrixes for DMB and PTMO. The subscript represents the bond number.

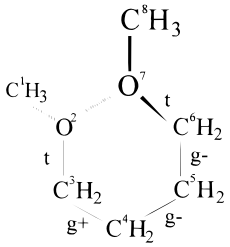

Figure 4. Example of 2,7-O···O interactions represented by the statistical weight ζ, found in the $tg^+g^-g^-t$ conformation of DMB. The interaction energy E_ζ was evaluated to be 0.738 kcal mol^{-1} by the ab initio MO calculations at the MP2/6-31+G*//HF/6-31G* (gas) level.

(cyclohexane) and J_T = 11.4 Hz and J_G = 4.4 Hz (DMSO); for $^3J_{\beta\gamma}$ and $^3J'_{\beta\gamma}$, J_T = 11.3 Hz and J_G = 4.9 Hz (cyclohexane) and J_T = 11.6 Hz and J_G = 4.7 Hz (DMSO). From the simulation for DMB, Inomata et al.[12] obtained J_T = 12.2 Hz and J_G = 3.3 Hz for $^3J_{\alpha\beta}$ and J_T = 13.6 Hz and J_G = 3.9 Hz for $^3J_{\beta\gamma}$ and $^3J'_{\beta\gamma}$. From NMR experiments for *tert*-butylcyclohexanols and substituted 1,3-dioxanes, Dale and Greig[17] estimated J_T = 11 Hz and J_G = 4 Hz for the C_α-C_β bond. For 1,3-dioxane, Buys and Eliel[18a] and Anteunis et al.[18b] determined the $^3J_{H4aH5a}$ and $^3J_{H4eH5a}$ values (corresponding to J_T and J_G respectively) to be 12.3−12.4 and 4.9 Hz, respectively. On the basis of the electronegativities of substituents, Phillips and Wray[19] have evaluated the vicinal coupling constants corresponding to those treated here: J_T = 13.07 Hz and J_G = 3.94 Hz for $^3J_{\alpha\beta}$ and J_T = 12.94−13.31 Hz and J_G = 3.63−4.44 Hz for $^3J_{\beta\gamma}$ and $^3J'_{\beta\gamma}$. For vicinal $-CH_2-CHX-$ (X = H, OCD_3, etc.) couplings, Haasnoot et al.[20] have presented empirical Karplus equations, from which J_T = 10.86−11.21 Hz and J_G = 4.26−4.71 Hz for $^3J_{\alpha\beta}$ and J_T = 13.03−13.33 Hz and J_G = 3.72−3.76 Hz for $^3J_{\beta\gamma}$ and $^3J'_{\beta\gamma}$ can be

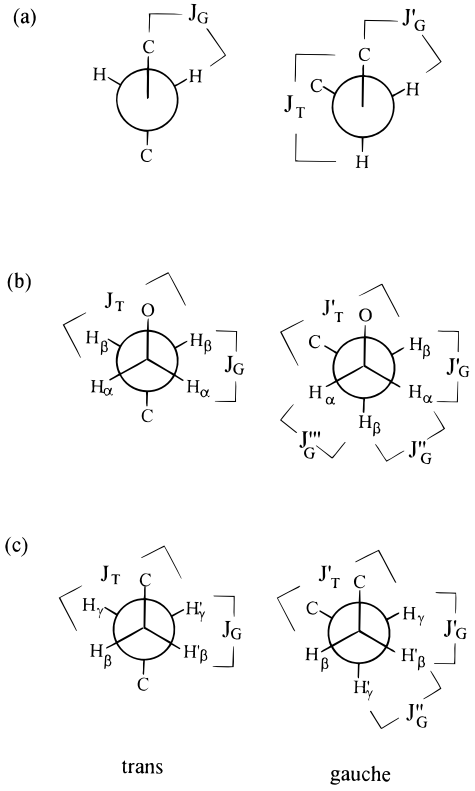

Figure 5. Preferred conformations and definition of the trans (J_T and J'_T) and gauche (J_G, J'_G, J''_G and J'''_G) vicinal coupling constants: (a) CO−CC (2 and 6), (b) OC−CC (3 and 5), and (c) CC−CC (4) bonds of DMB.

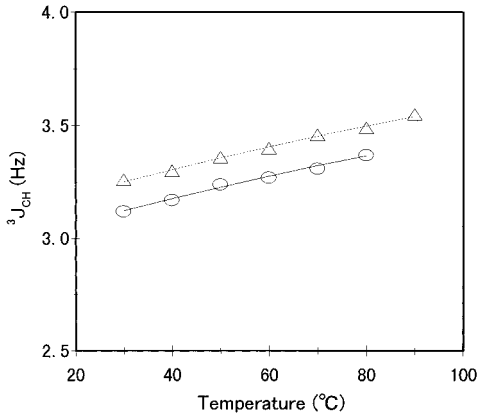

Figure 6. Temperature dependence of $^3J_{CH}$ for DMB. The open circle and triangle stand for observed values from the cyclohexane and dimethyl sulfoxide (DMSO) solutions, respectively.[12] The solid and dotted lines represent the calculated values from eq 1 for the cyclohexane and DMSO solutions, respectively.

derived. It can be understood that comparatively wide ranges of J_T and J_G have been evaluated and used for the $^1H-^1H$ coupling constants. Our simulations yielded the J_T and J_G values within the allowable ranges, despite the simplifications $J_T = J'_T$ and $J_G = J'_G = J''_G = J'''_G$ and neglect of the solvent effects on the conformational energies.

From the NMR vicinal coupling constants, on the other hand, Inomata et al.[12] have obtained the conformational energy set shown as "study III" in Table 1. It is thus difficult to consider the NMR data treated here to provide a stringent criterion for conformational energies of DMB and PTMO.

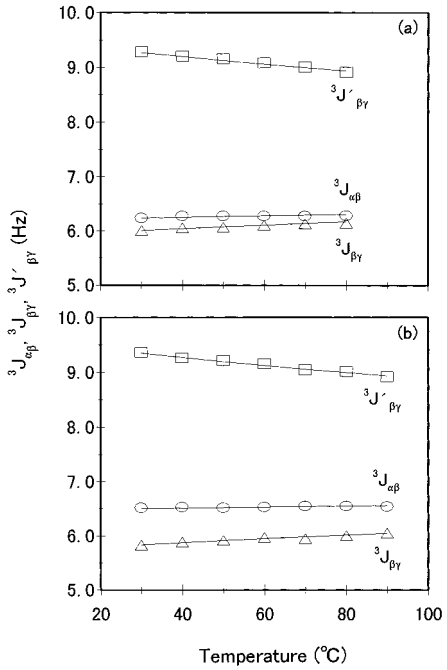

Figure 7. Temperature dependence of $^3J_{\alpha\beta}$, $^3J_{\beta\gamma}$ and $^3J'_{\beta\gamma}$ for DMB in (a) cyclohexane and (b) DMSO. The observed values (ref 12) are represented as follows: (○) $^3J_{\alpha\beta}$; (△) $^3J_{\beta\gamma}$; (□) $^3J'_{\beta\gamma}$. The solid lines stand for the corresponding calculations.

C−O Bond Dipole Moment[21]

In most of the conformational analyses of polyethers $[-(CH_2)_y-O-]_x$,[1-3,12,22-25] for the C−O bond dipole moment (m_{C-O}) values of 0.99 and 1.07 D have been employed and the C−C bond dipole moment (m_{C-C}) has always been assumed to be null. Recently, however, Smith et al.[26] have pointed out that the m_{C-O} value of 1.07 D is too small to reproduce the dipole moments obtained by their ab initio MO calculations at the MP2/D95+(2df,p) level for conformers of 1,3-dimethoxypropane and recommended use of m_{C-O} = 1.16 D instead. Thus we have attempted to determine the m_{C-O} value of polyethers from the MO[7] and ^1H NMR[27] data for 1,2-dimethoxypropane (1,2-DMP).

In the previous study[7] we have calculated the dipole moments $<\mu>$ of 1,2-DMP and the dipole moment ratios $\langle\mu^2\rangle/nm^2$ of PPO using the conformational energies obtained from ab initio MO calculations with the self-consistent reaction field (SCRF) method.[28] The SCRF calculation is used for estimation of the electronic properties perturbed by solvents. For the benzene solutions, however, the agreement in $\langle\mu\rangle$ and $\langle\mu^2\rangle/nm^2$ between theory and experiment was unsatisfactory. This is probably because the SCRF calculations failed to yield accurate conformational energies for the benzene solution. The bond conformations of the central C−C bond of 1,2-DMP, evaluated from the NMR $^1H-^1H$ coupling constants,[27] were shown to exhibit remarkable solvent dependence: the gauche stability has a tendency to be enhanced with increasing solvent polarity. The MO calculations could not reproduce the solvent dependence well.

First, therefore, we have partly altered the conformational energies obtained from the MO calculations so as to accord the calculated C−C bond conformations exactly with those determined from the NMR experiments. The conformation of the C−C bond (bond 3, see Figure 8) was, in particular, found to be sensitive to the

Table 2. Conformational Energies of 1,2-DMP, Evaluated from ab Initio MO Calculations and ^{1}H-NMR Data[a]

	gas		cyclohexane		benzene		dimethyl sulfoxide	
	MO	NMR	MO	NMR	MO	NMR	MO	NMR
				First-Order Interaction				
E_α	0.714	0.77 ± 0.04	0.527	0.71 ± 0.00	0.502	0.54 ± 0.03	0.238	0.26 ± 0.03
E_β	1.297	1.2 ± 0.1	1.171	1.1 ± 0.0	1.153	0.83 ± 0.04	0.896	0.41 ± 0.04
E_γ	3.057		2.979		2.967		2.813	
E_δ	0.352		0.238		0.223		0.029	
E_σ	1.516		1.419		1.406		1.256	
				Second-Order Interaction				
$E_{\omega1}$	−1.236		−1.064		−1.040		−0.787	
$E_{\omega2}$	−1.884		−1.768		−1.753		−1.536	
				Third-Order Interaction				
E_χ	−1.266		−0.948		−0.908		−0.480	

[a] In kcal mol^{-1}. For the definition of the conformational energies, see Figure 8. MO: obtained from ab initio MO calculations at the MP2/6-31+G*//HF/6-31G* level (ref 7). NMR: obtained using eqs 5−7. Then the bond conformations determined from the NMR vicinal ^{1}H-^{1}H coupling constants (ref 27) were used: for the gas phase, $p_{t;3} = 0.38 \pm 0.01$, $p_{g+;3} = 0.41 \pm 0.01$, and $p_{g-;3} = 0.21 \pm 0.01$ (145 °C); for the cyclohexane solution, $p_{t;3} = 0.41 \pm 0.00$, $p_{g+;3} = 0.41 \pm 0.00$, and $p_{g-;3} = 0.18 \pm 0.01$ (26 °C); for the benzene solution, $p_{t;3} = 0.34 \pm 0.01$, $p_{g+;3} = 0.44 \pm 0.01$, and $p_{g-;3} = 0.22 \pm 0.01$ (26 °C); for the dimethyl sulfoxide solution, $p_{t;3} = 0.26 \pm 0.01$, $p_{g+;3} = 0.43 \pm 0.01$, and $p_{g-;3} = 0.31 \pm 0.01$ (25 °C).

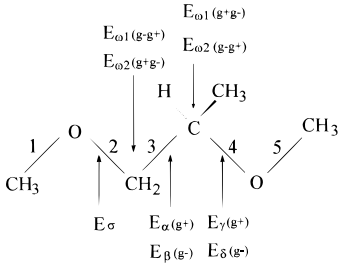

Figure 8. Schematic representation of (*R*)-1,2-dimethoxypropane (1,2-DMP) in its all-trans conformation. The bonds are numbered as indicated. The first-order interaction energies E_σ ($g^\pm$ of bond 2, relative to the corresponding t state), E_α (g^+ of bond 3), E_β (g^- of bond 3), E_γ (g^+ of bond 4), and E_δ (g^- of bond 4), the second-order $E_{\omega1}$ (g^-g^+ of C−O/C−C pairs) and $E_{\omega2}$ (g^+g^- of C−O/C−C pairs) and the third-order E_χ ($g^+g^+g^+$) have been defined for 1,2-DMP and poly(propylene oxide) (PPO), where the individual energies are assigned to the conformations in the parentheses. The statistical weight is given as the Boltzmann factor of the corresponding conformational energy.

solvent. Thus only the E_α and E_β values were adjusted with the other conformational energies fixed as obtained from the SCRF calculations. The bond conformations can be related to the statistical weights by

$$\frac{p_{g+;3}}{p_{t;3}} = \frac{1 + \sigma + \sigma\omega_1 + \gamma(1 + \sigma\chi + \sigma\omega_1) + \delta\omega_1(1 + \sigma)}{(1 + \sigma)(1 + \gamma + \delta)}\alpha \tag{5}$$

$$\frac{p_{g-;3}}{p_{t;3}} = \frac{1 + \sigma\omega_2 + \gamma\omega_2 + \delta(1 + \sigma\omega_2)}{(1 + \sigma)(1 + \gamma + \delta)}\beta \tag{6}$$

$$p_{t;3} + p_{g+;3} + p_{g-;3} = 1 \tag{7}$$

The definition of the statistical weights is shown in Figure 8. Substituting the experimental values of $p_{t;3}$, $p_{g+;3}$, and $p_{g-;3}$ and the theoretical values of E_γ, E_δ, E_σ, $E_{\omega1}$, $E_{\omega2}$, and E_χ into eqs 5−7, we determined the E_α and E_β values. The results are listed in Table 2.

From the table, it can be seen that the MO theory at the MP2/6-31+G*//HF/6-31G* level gives good data, at least, for the gas phase; the MO data agree closely with the semiempirical ones. The E_α (0.54 ± 0.03 kcal mol^{-1}) and E_β (0.83 ± 0.04 kcal mol) values obtained for the benzene solution are comparable with those (E_α = 0.4 and E_β = 0.6 kcal mol^{-1}) estimated using the molecular mechanics calculations of Abe et al.[4]

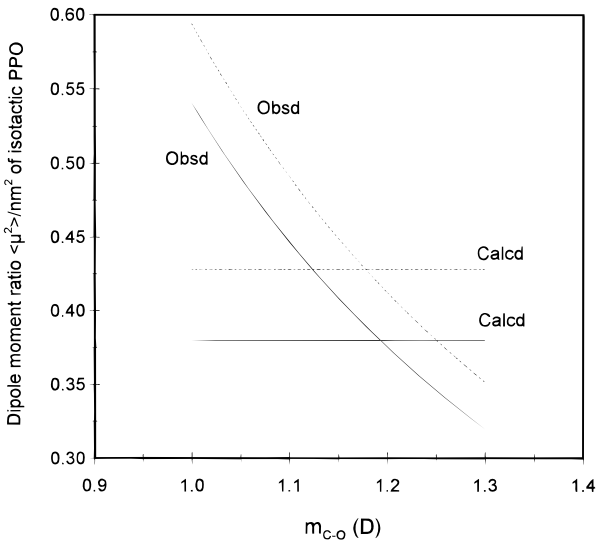

Figure 9. Dipole moment ratio of *isotactic* PPO as a function of C−O bond dipole moment (m_{C-O}). The $\langle\mu^2\rangle/nm^2$ values for the cyclohexane and benzene solutions at 25 °C were calculated to be 0.38 ± 0.00 and 0.43 ± 0.01, respectively, being represented by the horizontal lines: (—) cyclohexane; (···) benzene. The experimental data can be expressed as $1.04^2/(2m_{C-O}^2)$ (—, cyclohexane) and $1.09^2/(2m_{C-O}^2)$ (···, benzene). The intersection of the horizontal line and concave curve give the optimal m_{C-O} value: m_{C-O} = 1.19 ± 0.00 D for the cyclohexane solution; m_{C-O} = 1.17 ± 0.02 D for the benzene solution.

Next, using the conformational energies thus determined, we calculated the dipole moment ratios of *isotactic* PPO, as described previously.[7] Then the m_{C-C} value was set equal to 0 D. The $\langle\mu^2\rangle/nm^2$ values calculated for the cyclohexane and benzene solutions at 25 °C were found to be independent of m_{C-O} and obtained as 0.38 ± 0.00 and 0.43 ± 0.01, respectively. The experimental $\langle\mu^2\rangle/nm^2$ value can be estimated from the observed dipole moment per monomer (reported to be 1.04 and 1.09 for the cyclohexane and benzene solutions at 25 °C, respectively),[25] thus being given as a function of m_{C-O}: $1.04^2/(2m_{C-O}^2)$ (cyclohexane) and $1.09^2/(2m_{C-O}^2)$ (benzene). Both functions are graphically given in Figure 9. The intersection of the calculation (the horizontal line) and observation (the concave line) gives the optimal m_{C-O} value. The solid (cyclo-

Table 3. Calculated and Observed Values of Characteristic Ratio and Dipole Moment Ratio and Their Temperature Coefficients of PTMO

	$\langle r^2\rangle/nl^2$		$d(\ln\langle r^2\rangle)/dT \times 10^3$, K^{-1}		$\langle \mu^2\rangle/nm^2$		$d(\ln\langle \mu^2\rangle)/dT \times 10^3$, K^{-1}	
	calcd	obsd	calcd	obsd	calcd	obsd	calcd	obsd
this study	5.68[a]		−0.723[b]		0.421[c]		2.43[d]	
	5.63[e]							
	5.58[f]							
study I[g]	4.6−5.3		−1.3 to −1.2		0.5−0.6		1.0−1.5	
study II[h]	5.9−6.4		−1.0		0.48−0.51		1.6	
study III[i]	5.9		−0.71		0.54		0.76	
		5.38[j]		−1.33[k]		0.42[l]		2.7[m]
		4.99[n]				0.41[o]		1.8[p]
		5.78[q]						
		6.85[r]						
		5.12[s]						
		6.13[t]						
		5.58[u]						
		5.71[v]						

[a] At 30 °C. [b] At 60 °C. [c] At 20 °C. [d] At 20 °C. [e] At 40 °C. [f] At 50 °C. [g] Reference 2. [h] Reference 3. [i] Reference 12. [j] Reference 30. In ethyl acetate (22.7 wt %) and *n*-hexane (77.3 wt %) at 31.8 °C. [k] Reference 22. In cross-linked network at 60 °C. [l] Reference 22. In benzene at 20 °C. Reestimated with $m_{C-O} = 1.18$ D and $m_{C-C} = 0.0$ D. [m] Reference 22. In benzene at 20 °C. [n] Reference 30. In ethyl acetate at 30 °C. [o] Reference 23. In benzene at 20 °C. Reestimated with $m_{C-O} = 1.18$ D and $m_{C-C} = 0.0$ D. [p] Reference 23. In benzene at 20 °C. [q] Reference 30. In cyclohexane at 30 °C. [r] Reference 30. In benzene at 30 °C. [s] Reference 31. [t] Reference 32. In ethyl acetate (22.7 wt %) and *n*-hexane (77.3 wt %) at 30.4 °C. [u] Reference 32. In 2-propanol at 44.6 °C. [v] Reference 32. In diethyl malonate at 33.5 °C.

hexane) and dotted (benzene) lines are found to have their intersection at $m_{C-O} = 1.19 \pm 0.00$ D and 1.17 ± 0.02 D, respectively. The characteristic ratio $\langle r^2\rangle_0/nl^2$ of *isotactic* PPO was also calculated from the semiempirical energy set for the cyclohexane solution and obtained as 5.9. The experimental data for *isotactic* PPO in the θ state (isooctane, 50 °C) range from 5.75 to 6.59, and the average value is 6.01.[29] For the $\langle r^2\rangle_0/nl^2$ value, good agreement with experiment was attained. On these grounds, we have employed the average value $m_{C-O} = 1.18$ D in the analysis for PTMO.

Characteristic Ratio and Dipole Moment Ratio of PTMO

In calculations of the characteristics ratio and dipole moment ratio of PTMO, we have used our conformational energy set listed in Table 1 and the statistical weight matrixes shown in Figure 3. Since we would like to compare only the effects of the conformational energies on these configuration-dependent properties between the present and previous studies, we have employed the same geometrical parameters as Inomata et al.:[12] bond lengths, $l_{C-C} = 1.53$ Å and $l_{C-O} = 1.43$ Å; bond angles, $\angle COC = \angle OCC = \angle CCC = 111.5°$, dihedral angles, $\phi_{g\pm;2} = \phi_{g\pm;6} = \phi_{g\pm;a} = \phi_{g\pm;e} = \pm 100.0°$, $\phi_{g\pm;3} = \phi_{g\pm;5} = \phi_{g\pm;b} = \phi_{g\pm;d} = \pm 117.0°$, and $\phi_{g\pm;4} = \phi_{g\pm;c} = \pm 108.0°$. Here, e.g., $\phi_{g\pm;a}$ denotes the dihedral angles for the gauche± states of bond a. The degree of polymerization, x, was assumed to be 100. The m_{C-O} and m_{C-C} values were set equal to 1.18 and 0 D, respectively.

Dimensions of PTMO in solutions have been estimated from the viscosity and light scattering measurements for a variety of solvents at different temperatures (see Table 3). The experimental $\langle r^2\rangle/nl^2$ values range widely from 4.99 to 6.85, and the average is 5.69. Of them, as $\langle r^2\rangle_0/nl^2$ of PTMO in the θ solvent, values of 5.38 (in ethyl acetate (22.7 wt %) and *n*-hexane (77.3 wt %) at 31.8 °C)[30] and 6.13 (in the same mixed solvent at 30.4 °C)[32] have been reported. To cover the temperature range where the measurements were carried out, the characteristic ratios at 30, 40, and 50 °C were calculated and obtained as 5.68, 5.63, and 5.58, respectively. The dipole moment ratio at 20 °C was calculated to be 0.421. The corresponding experimental value was reported to be 0.41−0.42. It should be noted that these data were reestimated with $m_{C-O} = 1.18$ D. Both calculated $\langle r^2\rangle_0/nl^2$ and $\langle \mu^2\rangle/nm^2$ values are in good agreement with the observations.

We have attempted to estimate allowances of the conformational energies of PTMO from the experimental $\langle r^2\rangle_0/nl^2$ and $\langle \mu^2\rangle/nm^2$ data. Using the statistical weight matrixes of Figure 3, we calculated both ratios with one of the energy parameters changed and the others fixed at the values listed as "this study" in Table 1. The above-mentioned geometrical parameters were used. Figure 10 shows the calculated $\langle r^2\rangle_0/nl^2$ and $\langle \mu^2\rangle/nm^2$ values as a function of the energy parameters. The horizontal solid and dotted lines represent tolerances of the experimental $\langle r^2\rangle_0/nl^2$ and $\langle \mu^2\rangle/nm^2$ data, respectively. From the energy range satisfying both experimental $\langle r^2\rangle_0/nl^2$ and $\langle \mu^2\rangle/nm^2$ extents, we may determine allowances of the conformational energies as follows: $0.81 \le E_\rho \le 0.92$ kcal mol^{-1}, $-0.70 \le E_{\sigma 1} \le -0.64$ kcal mol^{-1}, $0.81 \le E_{\sigma 2} \le 0.88$ kcal mol^{-1}, $-0.43 \le E_\omega \le -0.19$ kcal mol^{-1}, and $0.57 \le E_\zeta \le 1.42$ kcal mol^{-1}. For the first-order interaction energies E_ρ, $E_{\sigma 1}$, and $E_{\sigma 2}$, the allowances are comparatively small. Increasing the order of interaction, however, allows a wider range of energy values. This is because conformers having the second- (E_ω) or third-order (E_ζ) interaction are less populated and less effective on the ensemble average. It is noteworthy that $E_{\sigma 1}$ and E_ω are shown to be still negative.

Conformational Characteristics and Crystal Structures of Polyethers $[-(CH_2)_y-O]_x$ ($y \ge 4$)

The crystal structure of PTMO was determined by Imada et al.[33] and Cesari et al.[34] Although bond b of PTMO has been indicated to prefer the gauche conformation in the θ state, the PTMO chain was found to take all-trans zigzag conformation in the crystal. This is probably because the PTMO molecule in the all-trans conformation can be packed more densely. Two molecular chains pass through the center and the corner of the monoclinic unit cell. The zigzag planes are parallel to each other and also to the *bc* plane of the unit cell. Thus the molecular arrangement is different from that

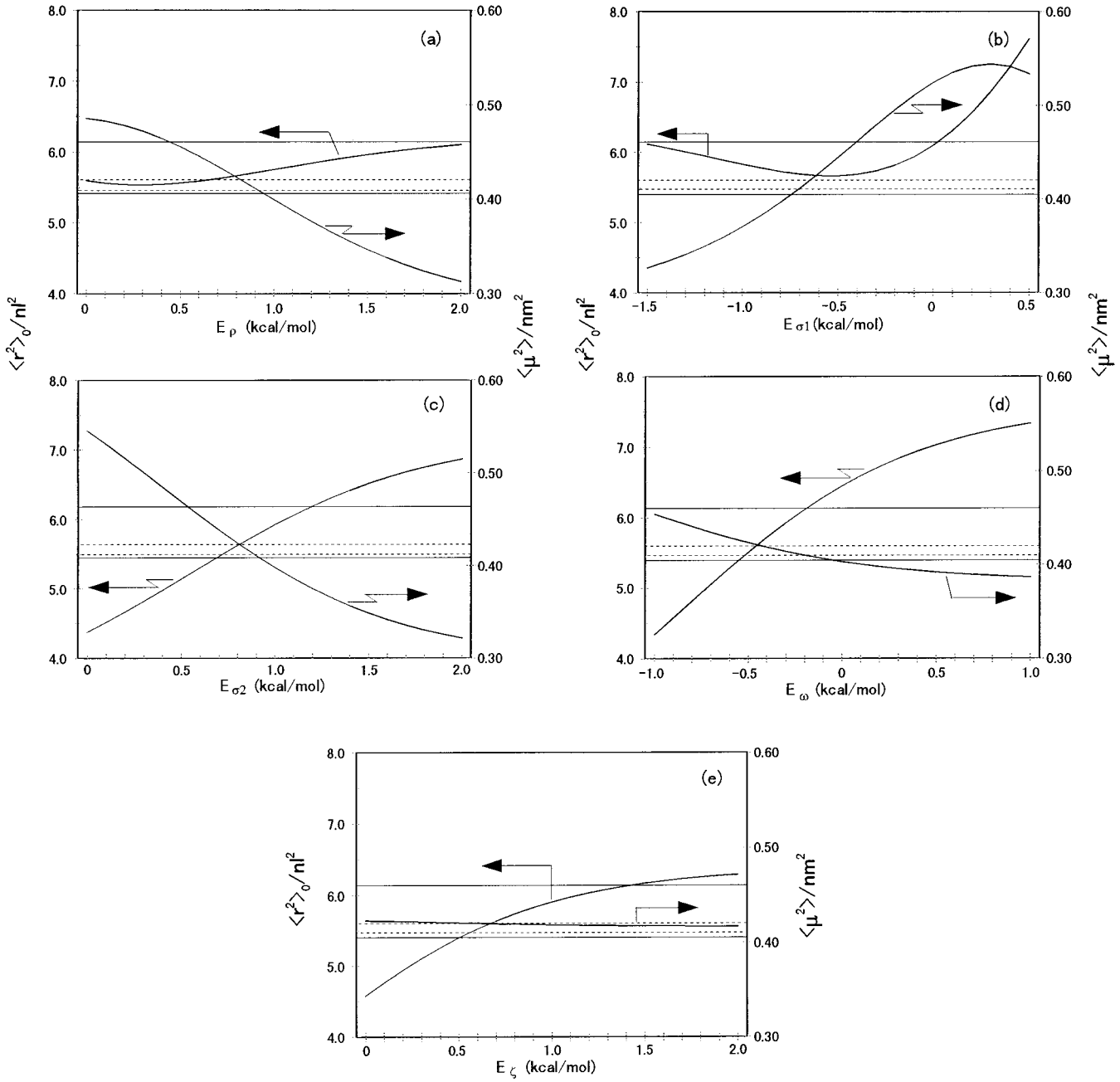

Figure 10. Allowances of the conformational energies of PTMO, estimated from the observed characteristic ratio and dipole moment ratio: (a) E_ρ, (b) $E_{\sigma 1}$, (c) $E_{\sigma 2}$, (d) E_ω, and (e) E_ζ. The thick solid curves stand for the calculated $\langle r^2\rangle_0/nl^2$ and $\langle \mu^2\rangle/nm^2$ values. The horizontal solid and dotted lines represent ranges of the experimental $\langle r^2\rangle_0/nl^2$ and $\langle \mu^2\rangle/nm^2$ values, respectively: 5.38 (ref 30) $\leq \langle r^2\rangle_0/nl^2 \leq$ 6.13 (ref 32) and 0.41 (ref 23) $\leq \langle \mu^2\rangle/nm^2 \leq$ 0.42 (ref 22).

of polyethylene (PE),[35] whose zigzag planes make an angle of 41° with the *bc* plane of the orthorhombic cell. The oxygen atoms of the neighboring molecules are not placed on the same level; the two molecular chains are shifted from each other so that the lone electron pair of the oxygen atom would be located close to the CH_2 group adjacent to the oxygen of the other molecule. These facts may suggest the presence of some *intermolecular* attraction between the oxygen and methylene group. By the Mulliken population analysis[36] based on the MP2/6-31+G*//HF/6-31G* (gas) calculation, the partial charges on the oxygen atom and its adjoining methylene group of the all-trans conformation of DMB were estimated to be −0.45 and +0.29, respectively (cf. for the $g^{\pm}g^{\mp}$ conformations for the C−C/C−C bond pair, −0.41 (O) and +0.19 (CH_2)[8]).

Extensive studies[33,37] on the crystal structure of a series of polyethers $[-(CH_2)_y-O]_x$ (y = 6, 8, 10, and 12) have been carried out and revealed the following facts. When poly(hexamethylene oxide) (y = 6) and poly(octamethylene oxide) (y = 8) are crystallized from the melt, they have a crystal structure of the PTMO type. However, crystallization from an ethanol solution leads the two polymers into a unit cell of the PE type. In general, the PE structure becomes more stable as y increases; poly(decamethylene oxide) (y = 10) and poly(dodecamethylene oxide) (y = 12) were found to form the PE structure even from the melt. The above tendencies may be interpreted in terms of the *intermolecular* (C−H)···O hydrogen bonding. The stabilization energy per monomeric unit, due to the (C−H)···O interaction, would decrease with increasing y. Thus the

polyether with a large y takes the PE structure, where the molecular chains are more closely packed. If ethanol molecules interact selectively with the $-CH_2-O-$ part of the polyethers, the residual solvents would prevent the polymeric chains from forming the intermoleuclar (C−H)···O hydrogen bond during crystallization. Then, even poly(hexamethylene oxide) and poly(octamethylene oxide) would take the PE structure.

Concluding Remarks

As shown above, the conformational energies obtained for DMB from the MO calculations at the MP2/6-31+G*//HF/6-31G* (gas) level satisfactorily reproduced the configuration-dependent properties available for both DMB and PTMO, even though no particular attention has been paid to the solvent effects.

The polyethers comprise only carbon, hydrogen, and oxygen atoms linked to one another only by single bonds. Despite their simple composition and structure, we must wait for the sophisticated MO calculations, at least, at the MP2 level to understand their conformational characteristics. Therefore, we should revisit conformational analyses of polymers containing other heterogeneous atoms such as halogens, nitrogen, sulfur, silicon, etc. to reveal the true structural features. The RIS scheme[14] has been shown to be still valid for predicting physical properties of unperturbed polymers.

References and Notes

(1) Mark, J. E.; Flory, P. J. *J. Am. Chem. Soc.* **1966,** *88,* 3702.
(2) Mark, J. E. *J. Am. Chem. Soc.* **1966,** *88,* 3708.
(3) Abe, A.; Mark. J. E. *J. Am. Chem. Soc.* **1976,** *98,* 6468.
(4) Abe, A.; Hirano, T.; Tsuruta, T. *Macromolecules* **1979,** *12,* 1092.
(5) Tsuzuki, S.; Uchimaru, T.; Tanabe, K.; Hirano, T. *J. Phys. Chem.* **1993,** *97,* 1346.
(6) Smith, G. D.; Yoon, D. Y.; Jaffe, R. L. *Macromolecules* **1993,** *26,* 5213.
(7) Sasanuma, Y. *Macromolecules* **1995,** *28,* 8629.
(8) Law, R. V.; Sasanuma, Y. *J. Chem. Soc., Faraday Trans.* **1996,** *92,* 4885.
(9) The abbreviation MP2/6-31+G*//HF/6-31G* (gas) represents the ab initio MO calculation carried out for a gaseous molecule (gas) by the following procedure: (1) the geometrical optimization by the Hartree−Fock (HF) calculation with the 6-31G* basis set; (2) the Hartree−Fock calculation followed by up to the second-order Møller−Plesset correlation energy correction (MP2) with the 6-31+G* basis set.
(10) To minimize the basis set superposition error,[11] we calculated the conformational free energies of DMB using basis sets larger than 6-31+G* and still obtained negative E_ω values. For details, see ref 8.
(11) van Duijneveldt, F. B.; van Duijneveldt-van de Rijdt, J. G. M.; van Lenthe, J. H. *Chem. Rev.* **1994,** *94,* 1873.
(12) Inomata, K.; Phataralaoha, N.; Abe, A. *Comput. Polym. Sci.* **1991,** *1,* 126.
(13) See, e.g.: Juaristi, E. *Introduction to Stereochemistry and Conformational Analysis*; Wiley: New York, 1991; Chapter 18.
(14) Flory. P. J. *Statistical Mechanics of Chain Molecules*; Interscience: New York, 1969.
(15) Xu, J.; Song, X.; Zhou, Z.; Yan, D. *J. Polym. Sci., Polym. Phys. Ed.* **1991,** *29,* 877.
(16) Marquardt, D. W. *J. Soc. Ind. Appl. Math.* **1963,** *11,* 431.
(17) Dale, J.; Greig, D. G. T. *Acta Chem. Scand.* **1974,** *B28,* 697.
(18) (a) Buys, H. R.; Eliel, E. L. *Tetrahedron Lett.* **1970,** 2779. (b) Anteunis, M. J. O.; Tavernier, D.; Borremans, F. *Heterocycles* **1976**, *4,* 293.
(19) Phillips, L.; Wray, V. *J. Chem. Soc., Perkin Trans. 2* **1972**, 536.
(20) Haasnoot, C. A. G.; de Leeuw, F. A. A. M.; Altona, C. *Tetrahedron* **1980**, *36,* 2783.
(21) The characteristic ratio and dipole moment ratio are expressed as $\langle r^2\rangle/nl^2$ and $\langle\mu^2\rangle/nm^2$ respectively, where $\langle r^2\rangle$ is the mean square end-to-end distance, $\langle\mu^2\rangle$ the mean square dipole moment, n the number of skeletal bonds, l^2 the average of square bond lengths, and m^2 the average of square bond dipole moments. The subscript 0 attached to $\langle r^2\rangle$ is indicative that the polymeric chain is in the θ state.
(22) Bak, K.; Elefante, G.; Mark, J. E. *J. Phys. Chem.* **1967,** *71,* 4007.
(23) Riande, E. *Makromol. Chem.* **1977,** *178,* 2001.
(24) Mark, J. E.; Chiu, D. S. *J. Chem. Phys.* **1977,** *66,* 1901.
(25) Hirano, T.; Khanh, P. H.; Tsuji, K.; Sato, A.; Tsuruta, T.; Abe, A.; Shimozawa, T.; Kotera, A.; Yamaguchi, N.; Kitahara, S. *Polym. J.* **1979,** *11,* 905.
(26) Smith, G. D.; Jaffe, R. L.; Yoon, D. Y. *J. Phys. Chem.* **1996,** *100,* 13439.
(27) Sasanuma, Y. *J. Phys. Chem.* **1994,** *98,* 13486.
(28) Wong, M. W.; Frisch, M. J.; Wiberg, K. B. *J. Am. Chem. Soc.* **1991,** *113,* 4776.
(29) Allen, G.; Booth, C.; Price, C. *Polymer* **1967,** *8,* 397.
(30) Kurata, M.; Utiyama, H.; Kamada, K. *Makromol. Chem.* **1965,** *88,* 281.
(31) Elias, H. G.; Adank, G. *Makromol. Chem.* **1967,** *103,* 230.
(32) Evans, J. M.; Huglin, M. B. *Makromol. Chem.* **1969,** *127,* 141.
(33) Imada, K.; Miyakawa, T.; Chatani, Y.; Tadokoro, H.; Murahashi, S. *Makromol. Chem.* **1965,** *83,* 113.
(34) Cesari, M.; Perego, G.; Mazzei, A. *Makromol. Chem.* **1965,** *83,* 196.
(35) Bunn, C. W. *Trans. Faraday Soc.* **1939,** *35,* 482.
(36) Mulliken, R. S. *J. Chem. Phys.* **1955,** *23,* 1833.
(37) Kobayashi, S.; Tadokoro, H.; Chatani, Y. *Makromol. Chem.* **1968,** *112,* 225.

MA971234E